RAPID COMMUNICATIONS

PHYSICAL REVIEW B VOLUME 50, NUMBER 11 15 SEPTEMBER 1994-I

Resonant tunneling through donor molecules

A. K. Geim, T. J. Foster, A. Nogaret, N. Mori, P. J. McDonnell, N. La Scala, Jr., P. C. Main, and L. Eaves
Department of Physics, University of Nottingham, Nottingham NG7 2RD, England
(Received 15 June 1994)

We discuss the origin of zero-dimensional states, which give rise to resonant structure at the current onset in tunneling devices. The states can be identified as being due to random pairs of shallow donors.

When the accuracy of measurements allows the detection of the passage of a single-electron current, a pronounced resonant structure is normally observed in the current-voltage characteristics $I(V)$ of tunneling devices. The additional resonances have been attributed to tunneling through random "impurity-related" states.[1–4] The number of these impurity states may be successfully controlled by careful design of GaAs resonant-tunneling devices (RTD's).[3,5] The technique is an alternative to the nanofabrication of quantum dots[6] and provides strongly confined zero-dimensional (0D) states. It offers a unique opportunity for detailed investigations of both the tunneling process through a single-impurity state and the local properties of a two-dimensional electron gas (2DEG) on a nanometer spatial scale. We have previously employed these self-assembled 0D states for studying many-body phenomena in resonant tunneling.[7] However, the microscopic origin of the 0D objects has remained unexplained. The detected 0D states are significantly deeper than the shallow donors, which one would expect in GaAs devices due to intentional or background doping.[2–4]

In this paper we show that the states are due to random clusters of shallow donors. We present studies of (AlGa)As double-barrier RTD's with intentional Si δ doping in the quantum well, and show that the number of subthreshold resonances increases with increasing doping level and device area. Also, deeper and deeper states appear as the number of Si donors in the RTD's increases. The average donor separation in our devices is much larger than the Bohr radius ($a_B \cong 10$ nm), which determines the scale when neighboring donors lead to electron levels appreciably deeper than for isolated donors. However, there is always a statistical probability of finding some of the donors at distances much smaller than average. The number of these pairs is relatively small but they can dominate the tunneling when other, more numerous states, remain out of resonance. We have calculated the current in the regime of tunneling through a random distribution of donor pairs ("hydrogenic molecules"[8]) and found good agreement with experimental $I(V)$. We also show that random donors in the contact regions may strongly influence states in the quantum well, contributing to the deep-level structure near the threshold.

The double-barrier RTD's were fabricated in square mesas of side lengths varying from 5 to 100 μm. The thickness of both $(Al_{0.4}Ga_{0.6})As$ barriers is 5.7 nm, the quantum well width w is 9 nm, and there is a 20-nm undoped spacer layer between each barrier and the doped contact regions. The doping starts from a low value (2×10^{16} cm^{-3}) over a thickness of 300 nm close to the spacer layers. We estimate the background impurity concentration in our structures to be $3–5\times10^{14}$ cm^{-3}. We also employed samples in which the center plane of the well was δ doped with Si donors at concentrations $n=2$, 4, and 8×10^9 cm^{-2}. The average donor separation in the well ranges from ≈0.1 μm ($n=8\times10^9$ cm^{-2}) up to ≈0.5 μm (undoped). Figure 1 shows a schematic energy-band diagram for a typical RTD under bias together with an $I(V)$ for a device with 8×10^9 cm^{-2} donor concentration. Tunneling occurs when a state in the quantum well comes in resonance with the 2DEG formed in an accumulation layer near the emitter barrier. The main resonance due to the lowest 2D subband in the quantum well has a large peak-to-valley ratio (20:1) indicating the high quality of our structures. At biases below the threshold for the main resonance a broad peak is observed with the maximum at 90 mV and the onset at ≈65 mV.[5] The peak amplitude increases linearly with increasing Si concentration in the well and the device area. The peak is due to tunneling through the single-donor (SD) level (Fig. 1) and its bias position is in good agreement with the binding energy of ≈12 meV for singly charged isolated donors near the center of the well.[9,5] For further details we refer to Refs. 3 and 5.

In Fig. 2 we show $I(V)$ of four different devices at biases

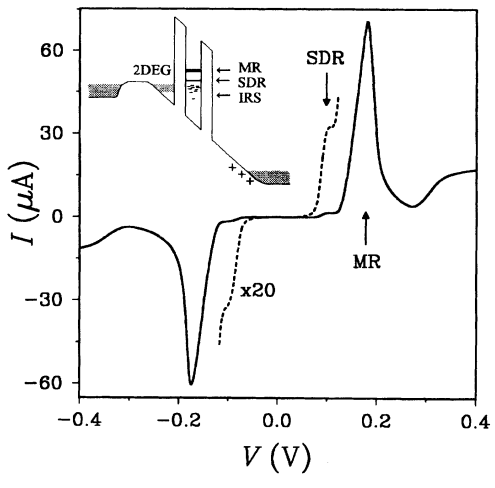

FIG. 1. $I(V)$ for a device 12 μm across with δ doping in the well 8×10^9 cm^{-2} at 1.3 K. The arrows show the main resonance (MR) and single-donor resonance (SDR). Dashed curve, 20× magnification of the SDR. The inset shows schematically the energy-band diagram for our RTD's under bias. The abbreviation IRS denotes impurity-related states.

0163-1829/94/50(11)/8074(4)/$06.00

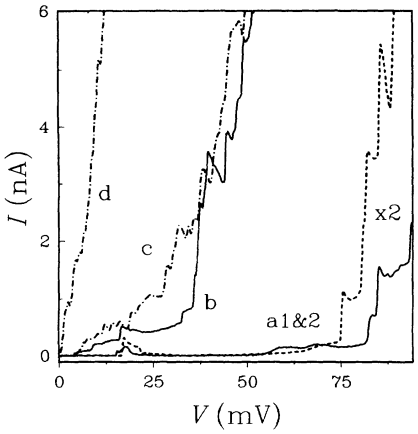

FIG. 2. Impurity-related resonances in four different devices at 0.3 K. $a1$ and $a2$, 12-μm-square undoped device at opposite biases; for clarity, the current scale is magnified by a factor of 2. b, undoped device 100 μm across. The dot-dashed curves are for devices 12 (c) and 100 μm (d) across with $n=4\times10^9$ cm^{-2}.

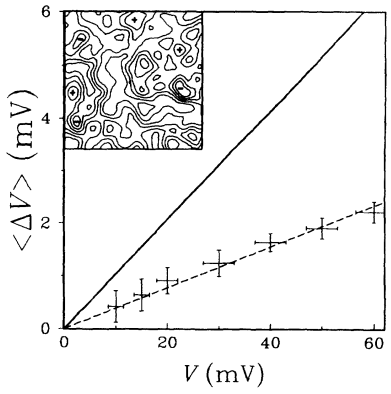

FIG. 3. Fluctuations ΔV in the voltage position of impurity resonances on reversal of bias direction. $\langle\Delta V\rangle$ denotes their rms amplitude. The dashed line is the best fit to experimental data (error bars). The inset plots equipotential lines (separation 1.4 meV) in the quantum well due to charged impurities in the collector contact at $V=50$ mV. +,− indicate some of the maxima and minima of the potential. The solid line is our model for $\langle\Delta V\rangle$ expected from the potential fluctuations.

below the onset of SD tunneling. Resonant structure is clearly seen on all the curves. Similar structure is observed in all devices, although details are unique to a particular device. For the undoped, small-area devices (curves a in Fig. 2), the current is usually zero (<0.1 pA) for biases up to about 60 mV. However, in some of the devices isolated peaks may occur such as that on curves a at $\approx$20 mV. The extra features in $I(V)$ become more extensive for larger device areas and with an increasing number of Si donors incorporated in the quantum well (curves b–d). The area and concentration dependence indicate that the impurity resonances are related to shallow donors in the well. However, the resonances occur at biases much lower than the SD resonance. Furthermore, the onset of the structure is not at a constant bias but shifts to lower biases as the device area or donor concentration increases (see Fig. 2). Note that the positions of the main and SD resonances remain unchanged in all devices. Binding energies of states can be calculated from their bias positions V.[3,7] Resonances near zero bias correspond to a binding energy of about 35 meV, much larger than the binding energy of an isolated Si donor in the well.[5,9]

Another feature in the behavior of impurity-related resonances is the dependence on bias direction. In our symmetric RTD's, resonances are expected to occur at the same voltage in both bias directions. This is true for the main and SD resonances (Fig. 1) but is not the case for subthreshold resonances. Although isolated resonant peaks always occur at similar values of V for both bias directions (e.g., see curves a in Fig. 2) and, hence, can be identified as the same impurity states in the well, the exact position of the resonances may shift significantly with bias direction. The observed shifts in voltage, $\Delta V=V_+-|V_-|$, were found to be random for any particular value of the mean bias $V=0.5\ (V_++|V_-|)$. In Fig. 3 we plot rms values of ΔV fluctuations at various applied voltages using data for more than 100 devices. The asymmetry in the position of impurity resonances is attributed below to potential fluctuations caused by the random distribution of donors in the doped contact regions.

The observed deep levels can be explained by pairs of Si donors situated in close proximity by random chance. In Fig. 4(a) we plot the electron binding energy ε_b to a donor pair (separation d) and to a triangle of three shallow donors (side d). The solid line represents ε_b of a donor pair in the 3D case [from Ref. 8(a)] while the dashed lines are calculations for hydrogenic donors in the 2D case,[8(b)] which are probably a better approximation for 10-nm quantum wells. As the separation decreases the binding energy increases. In the limit of zero separation, ε_b reaches the expected values of $Z^2\varepsilon_0$, where Z is the number of donors in the cluster and ε_0 is the single-donor binding energy. Even two donors separated by a_B give rise to a state 2.5–3 times deeper than an isolated donor and there are considerable changes in ϵ_b for separations as large as several a_B (see Fig. 4). Both models give generally the same functional dependence and, for clarity, we use below the 2D calculations unless stated otherwise.

An average donor in our devices can be regarded as isolated since the average donor separation is larger than a_B by more than an order of magnitude. This is in agreement with the constant bias position of the SD resonance in all our devices. On the other hand, donor separations much less than average can also occur. For a mesa area S and a sheet-donor density in the well n, the probability of finding a donor pair with separation d *or less* is given by[10]

$$P=1-\prod_{k=0}^{N-1}(1-k/z), \tag{1}$$

$z=-S/\pi d^2$, and $N=nS$ is the number of donors in the well. The probabilities P for the devices in Fig. 2 are plotted in Fig. 4(b), assuming a background concentration of 4×10^{14} cm^{-3} for the undoped devices. In particular, Eq. (1) implies that one can expect (with $P\approx0.5$) in any device one pair of donors with separation $d\leq d_2\approx1/n\sqrt{S}$. The isolated peak on curves a in Fig. 2 corresponds to a binding energy $\approx$30 meV, which requires a donor separation of about 5 nm in the 2D

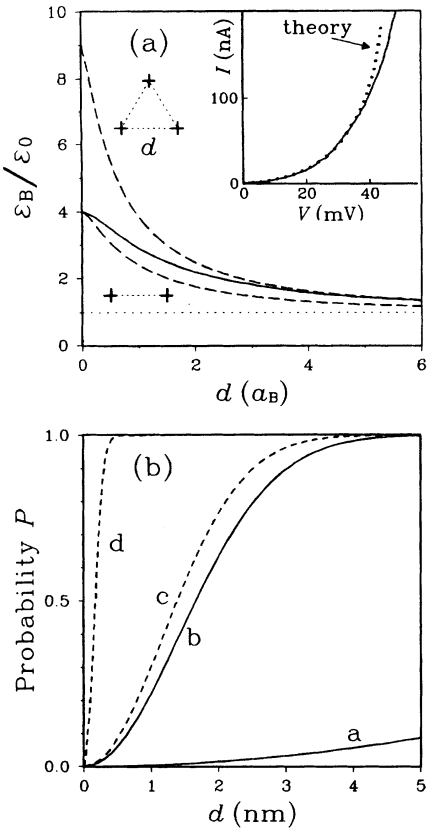

FIG. 4. (a) Binding energies ε_b of electrons to a pair and a triangle of shallow donors. Solid and dashed lines are for 3D and 2D cases, respectively. (b) Statistical probability of finding a pair of donors at a distance d or less in the devices $a-d$ of Fig. 2. Inset: comparison of our model (dots) with an experimental I-V (solid curve) in the regime of donor-pair tunneling.

case. The probability of finding such a pair in an undoped device 12 μm across is $\approx 10\%$ [Fig. 4(b)]. This agrees well with the fact that only a few among dozens of undoped small-area devices measured in our experiments have exhibited peaks at such low biases. In contrast, for 12-μm devices with donor concentration 4×10^9 cm^{-2} and 100-μm undoped devices, the onset of the current normally occurs close to (but still above) zero bias (curves b and c in Fig. 2). In these devices we may expect a donor pair with separation smaller than 2 nm and, hence, with binding energy very close to the energy of a doubly charged donor (see Fig. 4). For a 10-nm quantum well, the binding energy of such a donor sited in the center plane is 37 meV (Fig. 5), in agreement with the binding energy found for zero-bias resonances. For larger area and more heavily doped devices, clusters of three donors may start to play a role. However, clusters resembling the equilateral triangle shown in Fig. 4(a) are important only at very high levels of doping not employed in the experiment.

The above analysis allows us to describe the overall behavior of experimental $I(V)$ in the regime of tunneling through donor-pair states. To this end, we have calculated the statistical distribution of the binding energies of pairs in our devices. Each deep level gives rise to a single-electron current e/τ (τ is the tunneling time) and, therefore, the net

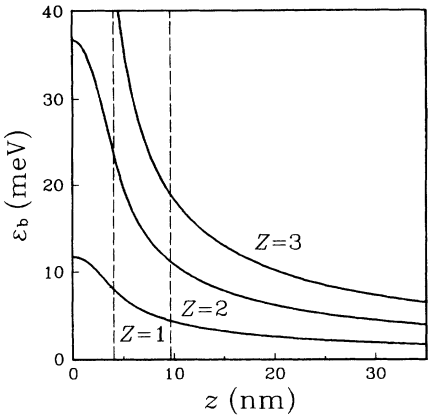

FIG. 5. Binding energy of an electron to a Z-charged donor vs the donor position z from the center of the quantum well. The dashed lines show the position of the barrier.

current at a particular bias is proportional to the number of pairs with the binding energy corresponding to that bias. The inset in Fig. 4(a) shows an example of a comparison between our model and the low-bias tail of $I(V)$ for device d in Fig. 2. Good agreement is found for $|V|\leq 40$ mV for this sample and for other devices where the number of donor pairs is large enough to avoid statistical fluctuations. The value of the single-electron current used in the calculations is ≈ 100 pA, consistent with a typical amplitude of subthreshold resonances.

To explain the asymmetry in the voltage position of resonances with respect to bias direction, we take into account the random distribution of impurities in the doped contact regions. Under bias, part of the collector contact becomes depleted (see inset in Fig. 1) and the charged, randomly distributed donors give rise to a fluctuating electrostatic potential in the quantum well.[11] The resonant energy of a strongly localized state in the well can fluctuate depending on whether the state is located in a maximum or minimum of this relatively smooth potential. Each bias direction has a different distribution of donors in the depleted layer, so the energy of a particular state may change randomly with a change in polarity. Therefore, ΔV is a measure of the amplitude of the potential fluctuations. Experimental data in Fig. 3 show that the rms amplitude $\langle \Delta V \rangle$ increases linearly with increasing applied bias in line with the increase in the number of unscreened donors in the collector. Note that although the concept of potential fluctuations due to remote Si donors is widely used for the case of a 2DEG in modulation-doped heterostructures,[11] no *direct* comparison between an experiment and theory has been possible.

We have simulated numerically the potential fluctuations in our devices and the results are shown in Fig. 3. Our model is similar to one described in Ref. 11. The width of the depleted collector layer and the number of charged donors in it are related to the voltage V through the capacitance of the structure. The donors are distributed randomly in this layer ($n=5\times10^{16}$ cm^{-3}), each giving a contribution to the potential in the well. The screening of the charged donors by electrons in the collector contact is modeled by an image charge placed symmetrically relative to the boundary of the depleted layer.[11] The screening by the more remote emitter 2DEG can

be neglected. The inset of Fig. 3 illustrates potential fluctuations in the quantum well in a 1×1-μm^2 area at 50-mV bias. The solid line in Fig. 3 shows the rms amplitude $\langle\Delta V\rangle$ calculated from such simulations of the potential fluctuations at different biases. No fitting parameters have been used. Our simulations are in qualitative agreement with the experiment, yielding $\langle\Delta V\rangle$ within a factor of 3 of the experimental values and the linear dependence on V. The difference in the absolute value of $\langle\Delta V\rangle$ is likely to be due to the rather simplistic model used to account for screening.

Finally, we note that the above model of potential fluctuations is expected to be valid only for the case of thick spacer layers. The density of charged donors in the depleted layer is rather large, leading to the likely presence of three-donor clusters at typical biases of a few tens of mV. These clusters give rise to resonant states in the quantum well, which can be even deeper than the SD level. Figure 5 plots the binding energy of a donor state in the well for various positions of the donor from the center of the well. In our devices with 20-nm spacer layers, a donor triplet in the collector leads to a resonant state with an energy ≈7 meV. This implies that clusters in the contacts cannot be responsible for subthreshold resonances in our devices, in agreement with the fact that the resonances appear for both bias directions.

In conclusion, a distribution of tightly bound states, responsible for the current onset of tunneling devices, is quantitatively explained by the presence of donor pairs with random separation. These "donor molecules" in the well and also in nearby contact regions can be important even for nominally undoped and small-area devices.

This work was supported by SERC (UK). L.E. and N.L.S. are grateful to the Royal Society (UK) and CNPq (Brazil), respectively, for financial support.

[1] J. Lambe and R. C. Jaklevic, Phys. Rev. **165**, 821 (1968); R. H. Koch and A. Hartstein, Phys. Rev. Lett. **54**, 1848 (1985); S. J. Bending and M. R. Beasley, *ibid.* **55**, 324 (1985); A. B. Fowler *et al.*, *ibid.* **57**, 138 (1986); T. E. Kopley *et al.*, *ibid.* **61**, 1654 (1988); M. V. Dellow *et al.*, *ibid.* **58**, 1754 (1992).

[2] T. W. Hickmott, Phys. Rev. B **46**, 15 169 (1992).

[3] J. W. Sakai *et al.*, Appl. Phys. Lett. **64**, 2563 (1994).

[4] M. A. Reed, Semicond. Sci. Technol. (to be published); M. Tewardt *et al.*, Solid State Electron. **37**, 793 (1994).

[5] J. W. Sakai *et al.*, Phys. Rev. B **48**, 5664 (1993).

[6] M. A. Reed *et al.*, Phys. Rev. Lett. **60**, 535 (1988); U. Meirav *et al.*, *ibid.* **65**, 771 (1990); B. Su *et al.*, Appl. Phys. Lett. **58**, 747 (1991); M. Tewordt *et al.*, Phys. Rev. B **45**, 14 407 (1992); P. Gueret *et al.*, Phys. Rev. Lett. **68**, 1986 (1992); R. C. Ashoori *et al.*, *ibid.* **68**, 3088 (1992).

[7] A. K. Geim *et al.*, Phys. Rev. Lett. **72**, 2061 (1994).

[8] (a) K. K. Bajaj *et al.*, J. Phys. C **8**, 530 (1975); (b) W. Kohm and J. M. Luttinger, Phys. Rev. **98**, 915 (1955).

[9] R. L. Greene and K. K. Bajaj, Solid State Commun. **45**, 825 (1983).

[10] P. I. Richards, *Manual of Mathematical Physics* (Pergamon, New York, 1959).

[11] J. A. Nixon and J. H. Davies, Phys. Rev. B **41**, 7929 (1990).

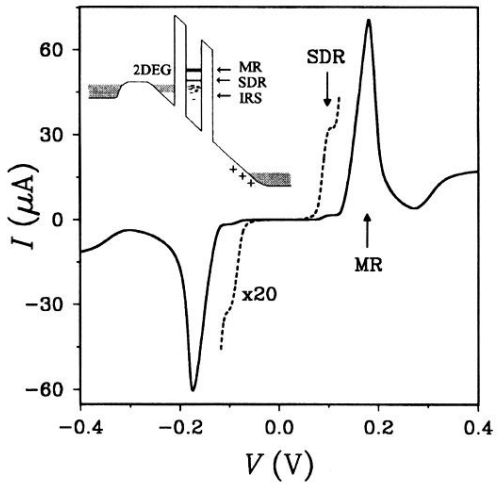

FIG. 1. $I(V)$ for a device 12 μm across with δ doping in the well 8×10^{9} cm^{-2} at 1.3 K. The arrows show the main resonance (MR) and single-donor resonance (SDR). Dashed curve, 20$\times$ magnification of the SDR. The inset shows schematically the energy-band diagram for our RTD's under bias. The abbreviation IRS denotes impurity-related states.